Ceramics-Silikáty 69 (3), 321-333 (2025)
www.ceramics-silikaty.cz doi: 10.13168/cs.2025.0016

ELECTROCHEMICAL ASSESSMENT OF REBAR CORROSION RESISTANCE IN GEOPOLYMER CONCRETE INCORPORATING GROUND GRANULATED BLAST FURNACE SLAG AND RICE HUSK ASH

#R. INDRAJITH KRISHNAN*, S. NAGAN**

*Department of Civil Engineering, Thiagarajar College of Engineering, Madurai, TamilNadu, India 625015
**Department of Civil Engineering, Thiagarajar College of Engineering, Madurai, TamilNadu, India 625015

#E-mail: jith@tce.edu

Submitted December 10, 2024; accepted March 1, 2025

Keywords: Chloride ion penetration, Electrochemical method, Open circuit potential, Linear polarisation resistance, Activator

The study mainly focuses on the development of a geopolymer concrete (GPC) to promote sustainable construction practices using agro-industrial by-products, specifically rice husk ash (RHA) and ground granulated blast furnace slag (GGBS). The primary aim of this research is to assess the resistance of GPC containing RHA and GGBS for corrosion, with specific attention to chloride-ingress corrosion, a significant durability concern for reinforced concrete structures in marine and industrial environments. The mix proportions used were 60 % RHA and 40 % GGBS. A blend of 12 M alkali activators was employed with sodium hydroxide solids and a sodium silicate solution. Tests, including the Rapid Chloride Ion Penetration Test (RCPT), Electrochemical methods, such as Linear Polarization Resistance test (LPR), and Open Circuit Potential test (OCP) were conducted to assess the chloride penetration and corrosion activity. The results indicate that corrosion risk decreases as the curing age increases, particularly in heat-cured specimens. The dense microstructure produced by GGBS enhances the resistance to chloride penetration, thus lowering the corrosion rates. GPC incorporating RHA and GGBS (RGGPC) shows superior corrosion resistance characteristics, making it a promising sustainable alternative.

INTRODUCTION

Geopolymer concrete (GPC) has recently gained remarkable attention as a sustainable alternative to Ordinary Portland Cement (OPC) concrete. This is primarily because geopolymer concrete has a lower carbon footprint and requires less energy during production, making it an environmentally friendly option [1, 2]. The term "geopolymer" encompasses a diverse group of engineered materials produced through a sequence of chemical reactions involving alumina-silicate sources and alkali activators [3, 4]. Geopolymer concrete possesses outstanding mechanical and durability properties [5, 6].

The deterioration of steel reinforcement bars placed into concrete is a significant issue that impacts the durability of reinforced concrete (RC) structures [7, 8]. While most concrete structures perform well even after a long period of use in normal environmental conditions, several reinforced concrete structures have experienced premature damage due to aggressive environmental conditions. The primary cause of rebar corrosion and the subsequent structural deterioration is chloride ion penetration into the concrete. In environments such as marine areas and industrial regions, the durability of concrete structures is crucial due to the continual exposure to aggressive environments [9]. Chloride ion penetrates the concrete through either larger pores and fissures or through diffusion in the smaller capillary pores of the paste, with diffusion serving as the prevalent mechanism. Diffusion takes place when the concentration of chloride on the outer surface of the concrete outdoes that on the inner surface, leading to the migration of chloride ions to reach the embedded rebar through the concrete [10].

Despite its potential benefits, the use of GPC in real-world applications is limited. This limitation arises primarily due to the need for more comprehensive data on its long-term durability, especially its effectiveness in protecting embedded reinforcement from corrosion [11]. Researchers have yet to fully explore how well GPC can withstand various environmental conditions over extended periods. Additionally, its ability to protect reinforcing steel within the concrete from corrosion remains an area that requires further investigation [12]. Some preliminary studies, especially those involving GPC exposed to marine environments, have shown that GPC can perform comparably to OPC concrete in resisting reinforcement corrosion.

Chloride ion penetration is a crucial aspect influencing the durability of GPC, particularly in aggressive environments such as marine or de--icing salt exposure. Studies like those by Ganesan [13] investigated the chloride diffusion characteristics of GPC made with 100 % fly ash (FA). The authors stated that the rate of chloride ion ingress in GPC is comparable to that of conventional concrete. These researchers employed AgNO3 spraying, a method recommended by ASTM C1556, to assess the depth and extent of chloride ion penetration. Conversely, Olivia [14] found that 100 % FA-based GPC revealed a greater rate of chloride penetration when compared to OPC concrete.

Similarly, Shayan [15] conducted rapid chloride permeability tests on 100 % slag-based GPC used in the construction of retaining walls in a bridge constructed across the Yarra River located in Melbourne, Australia, which had been in service for five years. The test results showed very low chloride permeability. Ma [16] also evaluated the chloride ion diffusion coefficient and corrosion rate of steel rebars placed in 100 % slag-based GPC and found that GPC revealed a lower chloride diffusion rate than OPC concrete. However, both materials showed comparable corrosion rates for the rebar. According to Wang et al. [17], the aluminate and silicate ions present in the alkali--activated slag (AAS) mortar result in the creation of a protective layer on the rebar. This effectively passivates the steel rebar compared to conventional cement mortars.

Tittarelli [18] examined the corrosion resistance behaviour of galvanised steel and bare steel as rebars in FA-based and metakaolin-based geopolymer mortars, comparing them to cement-based mortars. These materials were exposed to wet and dry cycles in a 3.5 % concentration of an NaCl solution. The experimental results indicated that FA-based geopolymers provided better protection for reinforcement due to their higher alkalinity, which delayed corrosion. However, due to the higher porosity, metakaolin-based geopolymers allowed a higher chloride ingress, increasing the corrosion, especially in galvanised steel. Overall, FA-based geopolymer mortars offered superior corrosion resistance to metakaolin-based and cement--based mortars. Gunasekara [19] reported that the chloride ion diffusion rate in GPC was influenced by the matrix's porosity, which depends on the fly ash reactivity. Additionally, the chloride bonding capacity of GPC was linked to the CaO content, which promotes the formation of C-A-S-H gel, reducing the chloride ingress. Tennakoon [9] found that FA-slag-based GPC had a lower chloride ion diffusion coefficient than traditional concrete and showed greater protection against corrosion of embedded rebar, even under chloride--contaminated conditions, compared to OPC concrete. These studies demonstrate that the corrosion behaviour of steel rebars in GPC is significantly influenced by the properties and types of source materials used, the molarity of the activator solution, and the overall mix design, curing conditions, and environmental exposure.

Despite the focus on materials like FA and GGBS in GPC durability studies, there has been limited research on other potential binder materials, such as rice husk ash (RHA), metakaolin, zeolite, and palm oil fuel ash. RHA, with its high silica content and excellent pozzolanic properties, could improve the performance of cementitious systems. However, RHA needs to be more utilised in developing GPC [20]. The lack of research on RHA's compatibility and long-term behaviour in GPC represents a significant gap in the literature.

The present research prepared a GPC mix comprising 60 % RHA and 40 % GGBS to address this gap. Various tests, including the Rapid Chloride Ion Penetration Test (RCPT), Linear Polarisation Resistance test (LPR), and Open Circuit Potential test (OCP), were conducted to evaluate the corrosion resistance behaviour of RHA and GGBS-based GPC (RGGPC). The study aims to demonstrate the potential of RHA as a viable source material for sustainable and durable GPC.

EXPERIMENTAL

Constituent materials

The materials used in this study include RHA, Ground granulated blast furnace slag (GGBS), alkaline activators, natural river sand as fine aggregate, crushed granite stone as the coarse aggregate, superplasticiser, and water.

RHA

The RHA was acquired from a rice mill in the southern district of Tamil Nadu, Madurai, which uses the fluidised bed method for combustion. The rice husk was burned at a controlled temperature of 700 °C for two hours, resulting in high-quality amorphous ash with a specific gravity of 2.13, as per IS 1393-1970,

Figure 1. Rice Husk Ash (RHA).

and a specific surface area of 655 $m^2 \cdot kg^{-1}$ measured using Blaine's air permeability apparatus. Figure 1 illustrates the RHA used in this study.

Characterisation of the RHA

- XRD Analysis: Figure 2 revealed highly amorphous RHA with poor crystalline SiO_2 growth.
- SEM Analysis: Figure 3 showed that the RHA particles are flaky with micropores, contributing to a higher specific surface area and water absorption.
- FTIR Analysis: The spectrum in Figure 4 indicated the presence of metal oxide bonds, with downward peaks at 1000 cm^{-1} confirming the absence of preformed bonds.

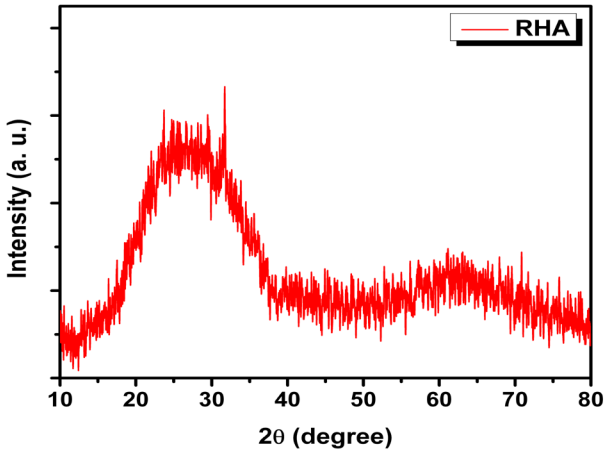

Figure 2. XRD for RHA.

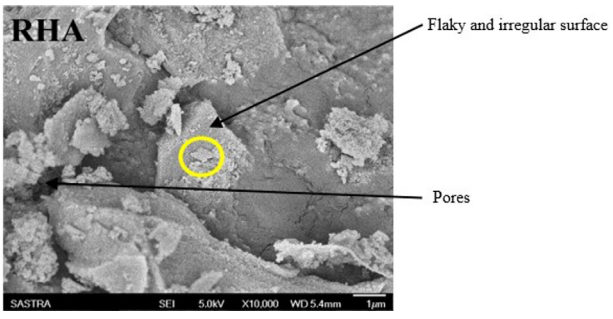

Figure 3. SEM image - RHA.

GGBS

GGBS, a residue generated from the iron smelting process, is illustrated in Figure 5 and has a specific gravity of 2.9 and a specific surface area using Blaine's apparatus test as 386 $m^2 \cdot kg^{-1}$.

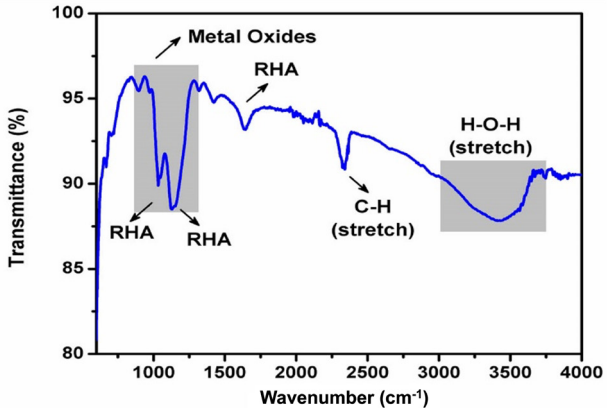

Figure 4. FTIR spectrum – RHA.

Figure 5. Ground granulated blast furnace slag.

Characterisation of the GGBS

- XRD Analysis: Figure 6 confirmed the amorphous nature of GGBS.
- SEM Analysis: Figure 7 revealed a layered, flake-like morphology without micropores, which enhances the strength.
- FTIR Analysis: Figure 8 presents the FTIR spectroscopy for GGBS. The region, spanning from 400 to 1400 cm^{-1}, exhibits complexity owing to the combination of the bending and stretching vibrations. The peaks corresponding to stretching vibrations indicate the presence of Al–O, Si–O, and carbonates, as also reported by Hassani [21]. The absence of peaks between 2000 cm^{-1} and 2500 cm^{-1} confirms the lack of C=C and C≡C bonds. The existence of the hydroxyl group is found at a peak of 3422 cm^{-1}, while the carbonate group is observed at a peak of 1493 cm^{-1}. The peak at 974 cm^{-1} results from the combined vibrations of Si–O and Al–O, and further, the observed peak at 714 cm^{-1} is attributed to the Al–O vibration.

The major oxide compositions of the RHA and GGBS obtained from the XRF techniques are detailed in Table 1.

Table 1. Chemical oxides for the RHA and GGBS.

Constituents	Chemical composition (%)	
	RHA	GGBS
SiO_2	91.45	34.91
Al_2O_3	0.7	17.82
Fe_2O_3	0.26	0.65
CaO	0.9	37.53
K_2O	1.87	0.54
P_2O_5	0.61	-
TiO_2	0.12	-
SO_3	0.04	0.24
Na_2O	-	0.2
MgO	-	7.91
MnO	-	0.2
LOI	4.03	-

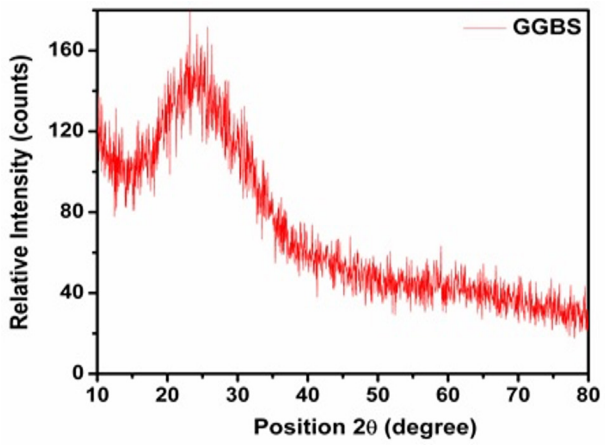

Figure 6. XRD - GGBS.

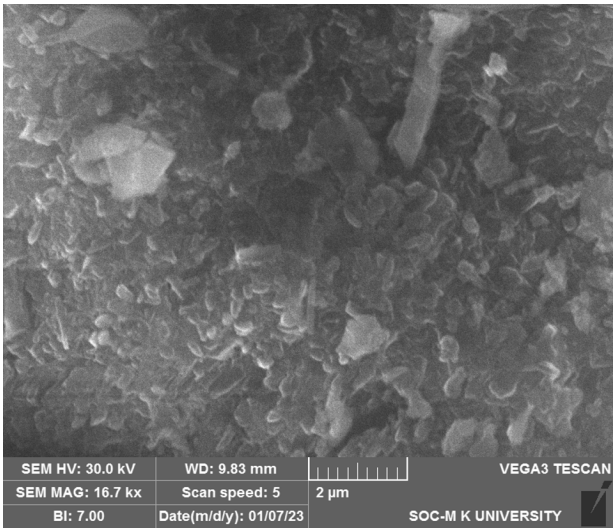

Figure 7. SEM image - GGBS.

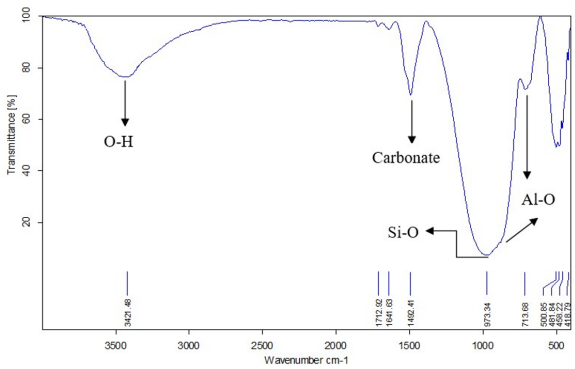

Figure 8. FTIR spectrum of the GGBS.

Aggregates and additives

The alkaline activator solutions used are sodium hydroxide (NaOH) in the form of flakes and sodium silicate (Na_2SiO_3) in a liquid form. The natural river sand, which has a specific gravity and fineness modulus of 2.63 and 2.66, respectively, is used as a fine aggregate, which falls under the Zone II grading in accordance with IS 383-2016. The coarse aggregate is crushed granite stone, tested according to IS 2386-1963 (part III), with a specific gravity of 2.76. The polycarboxylate ether--based superplasticiser has been utilised to produce RGGPC. These materials were chosen and characterised to confirm the quality and performance of the RGGPC mix, adhering to the relevant standards.

Mix proportioning, casting and curing of RGGPC

The mix design, meticulously proposed by Lloyd [22] was adopted to establish the mixture proportions for GPC, with the GPC density as 2400 kg·m^{-3} (assumed). The combined weight of FA and activator solution was calculated with precision by subtracting the aggregate quantity from the GPC density. Based on this, the RHA content was determined using an activator solution-to-binder component ratio of 0.5. The activator solution is a mixture of Na_2SiO_3 and NaOH, which was proportioned according to a ratio of 2.5.

The total aggregate content was considered 77 % by mass for this experimental study. The superplasticiser quantity was finalised at 1.5 % of the cementitious material's weight after successful trial mixes, within a permissible range of 0 to 2 %. Additional water, equal to 31.75 % weight of the binder was used to prepare the GPC with RHA, achieving the desired consistency through effective trial-and-error methods. A 12 M NaOH solution was used.

The coarse aggregate sizes of 20, 12 and 6 mm were combined in proportions of 15, 20 and 35 %, respectively, relative to the total aggregate (sand and coarse aggregate). Coarse aggregates constituted about 70 % of the total aggregate. The mix, containing 60 % RHA and 40 % GGBS as binder materials, is detailed in Table 2 and designated as R60G40.

Table 2. Mixture proportion of the RGGPC.

Constituents	Quantity (in kg·m^{-3})
RHA	184.80
GGBS	167.70
Sand	554.40
Coarse Aggregate	1293.60
Sodium Hydroxide Solution	52.57
Sodium Silicate Solution	131.43
Superplasticiser (% by weight of cementitious material)	1.50

A pan mixer machine was utilised to prepare the GPC specimens. The activator solution was prepared one day before the casting for better chemical reaction and to ensure bonding between the raw materials. The mixing process began with dry materials being mixed until a uniform consistency was achieved, followed by gradually adding the alkaline activator. Subsequently, the superplasticiser and extra water were incorporated, and mixing was continued for 10 to 15 minutes to achieve the desired workable mix.

The concrete mixture was carefully placed into moulds, and compaction was conducted using a vibrator. The specimens were cast within 15 minutes of mixing, ensuring their integrity. Once placed in the moulds, the specimens were left undisturbed until they reached the final set and were then stored at room temperature for 24 hours. After the specified period, the specimens were demoulded and subjected to two different curing methods: heat and ambient curing. In the ambient curing method, the specimens were exposed to ambient conditions at room temperature for the respective days of curing (30, 60 and 90 days). In contrast, the specimens were initially kept in a heat-curing chamber set at 60 °C for 24 hours for the heat-curing method. After this, they were kept at room temperature in open air for the same duration.

Test procedure

Workability, compressive strength and microstructure of RGGPC

The workability of the RGGPC mixture was assessed using the slump cone test, conducted as per IS 1199 (Part 2)-2018. The compressive strength was determined using 150 mm cubic specimens, following the guidelines of IS 516-1959. A microstructural study was performed on the fractured samples from the compressive strength test using SEM and FT-IR techniques.

Rapid chloride ion penetration

The durability of RC structures is significantly affected by their resistance to chloride ion penetration, as chloride ingress is a primary factor leading to steel reinforcement corrosion. The ability of concrete to resist the ingress of chloride ions is crucial for the longevity of structures, especially those exposed to harsh environments like coastal areas, where chloride ions are prevalent due to seawater or de-icing salts. The low permeability of concrete plays a crucial role in this resistance; the fewer pores in the concrete, the harder it is for chloride ions to penetrate the material and reach the steel reinforcement.

In the case of geopolymer concrete, which is made from industrial or agricultural by-products activated with an alkaline solution, there are some inherent advantages when it comes to chloride resistance. Geopolymer concrete generally has a denser microstructure and lower porosity than conventional concrete, resulting in a reduced permeability. These characteristics significantly reduce the pathways for chloride ions to penetrate, enhancing the material's durability and its resistance to corrosion.

The rapid chloride permeability test (RCPT) is widely used to evaluate the permeability of concrete to chloride ions. This test quantifies the total electrical charge (measured in Coulombs) passing through a concrete specimen over a fixed period, with lower Coulombs indicating better resistance to chloride penetration. The testing procedure followed in this study adhered to the guidelines specified in ASTM C1202-17. The specimens used for this test were discs, measuring 100 mm in diameter and 50 mm in height. Prior to testing, the concrete discs were thoroughly air-dried. To prevent water leakage in the specimen, the edges of the disc were applied with an epoxy sealant, after which they were kept in a desiccator, where both surfaces were exposed. The vacuum desiccator was then sealed and exposed to a 6.65 kPa vacuum pressure for a duration of three hours. Subsequently, distilled water was added to the desiccator, fully submerging the specimens, and the same pressure was maintained for another hour. After this period, the vacuum pump was switched off, and the specimens remained in the desiccator until the complete saturation of the specimen. Then, the specimens were transferred to a plexiglass reservoir and were sealed using silicone as a sealant. The positive end of the reservoir was filled with an NaOH solution of 0.3 Normality, while the negative end was filled with a 3.0% NaCl solution. A direct current of 60 V potential was supplied across the specimen, and the current flow was measured for six hours at 30-minute intervals. The total electric charge transmitted through the disc was estimated from the formula provided by ASTM C1202-17, and the concrete quality was evaluated based on the criteria provided in the standard.

Corrosion resistance of RGGPC

The corrosion of reinforcing bars (rebars) in concrete is a key issue that effects the long-term durability of structures. Concrete naturally protects steel reinforcement because it creates an alkaline environment around the steel, which forms a protective coating called the passive layer. This layer keeps the steel from rusting under normal conditions. However, when concrete is exposed to harsh conditions, especially in environments with high levels of chloride ions (like seawater or de-icing salts), these ions can travel through the concrete and reach the steel bars inside. Once the chloride ions make their way to the steel, they break down the protective layer that keeps the steel from rusting. This leads to rust formation, which makes the steel rebars expand, and eventually, the concrete cracks and starts to break apart, further exposing the steel to damage. The ability of concrete to resist this type of corrosion largely depends on its effectiveness in preventing harmful chloride ions from penetrating the steel.

Various techniques are used to measure the corrosion resistance of rebars, either by assessing the material's properties or by monitoring corrosion activity in service. These techniques can be broadly categorised into electrochemical, non-destructive, and accelerated laboratory methods. In this study, the electrochemical methods such as Open Circuit Potential (OCP) and Linear Polarisation Resistance (LPR) tests were carried out to assess the likelihood of corrosion and corrosion rate in steel rebars embedded in RGGPC. The test procedure is summarised below.

Conditioning of the test specimens

Cylindrical specimens (of size 100 mm diameter and 200 mm height) reinforced with a 10 mm diameter rebars, were cast to evaluate the corrosion resistance behaviour of RGGPC specimens. The steel rebar was placed centrally within each cylinder, ensuring a 20 mm cover at the bottom. For both the OCP and LPR tests, eighteen specimens were cast for both curing conditions. After the specified curing age, the cast specimens were thoroughly immersed in a NaCl solution of 3.5 % concentration and exposed to 2 cycles of wetting and drying to accelerate the corrosion process. Each cycle involves a week of wetting followed by a week of drying. Figure 9 shows the specimens in the NaCl solution.

Figure 10 illustrates the test set-up used for the experimental evaluation. A silver chloride electrode, a platinum electrode, and a rebar were used as the reference, counter, and working electrode, respectively, in both OCP and LPR tests. These electrochemical tests were carried out using an electrochemical workstation.

Figure 9. Test specimens in an NaCl solution.

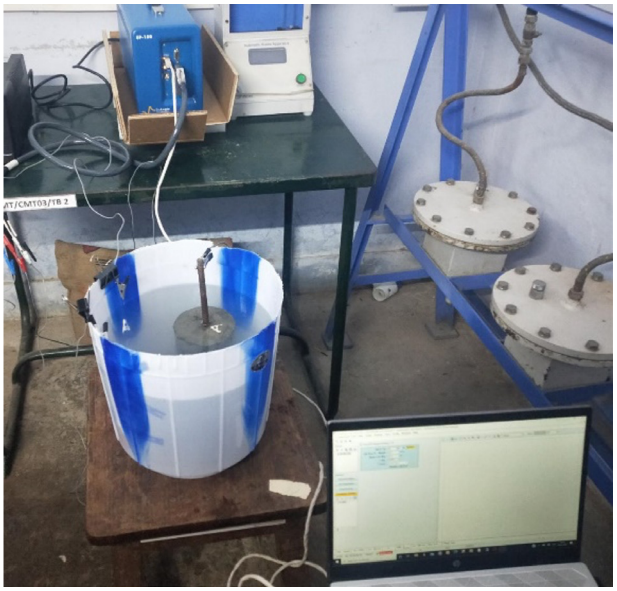

Figure 10. Corrosion evaluation – test set-up.

Open circuit potential test

The OCP test followed the standards specified in ASTM C876-15. The corrosion potential, represented as Ecorr, indicates the voltage difference between the rebar and a reference electrode, reflecting the condition of the steel rebar within the environment. The direct measurement of Ecorr on the steel surface is not feasible; instead, it must be assessed through the concrete cover, which acts as an electrolyte.

The potential of the steel reinforcement relative to the reference electrode was measured, and these values were analysed as per the criteria provided in ASTM C876-15 to determine the corrosion risk probability.

Linear polarisation resistance test

One of the most extensively used techniques for estimating the corrosion rate is the LPR method. Polarisation occurs when the applied potential shifts the steel rebar potential away from its open circuit potential, inducing a current. The resulting induced current is found and analysed to study the corrosion behaviour of the rebars. The corrosion rate can be estimated using polarisation resistance (R_p), which can either be experimentally measured or calculated.
The corrosion rate is evaluated using the mathematical equation as per ASTM G59-97 given below.

$$Corrosion\ rate = 3.27\times10^{-3}\times i_{corr}\times\frac{EW}{\rho} \qquad (1)$$

where β_a and β_c are anodic and cathodic Tafel slopes obtained from polarisation plot, EW is the equivalent weight of the rebar, i_{corr} is the corrosion current density ($\mu A \cdot cm^{-2}$) and ρ is the density of the rebar in $g \cdot cm^{-3}$.

A three-electrode system is used in the LPR test. The steel rebars, silver/silver chloride (Ag/AgCl), and platinum electrode act as the working, reference, and counter electrodes. During the experiment, the steel rebars are subjected to a controlled potential scan of ± 25 mV around the open circuit potential. The data collected from this scan generates a plot of the resulting current versus applied potential. These plots are then analysed to extract key electrochemical parameters such as corrosion current density (i_{corr}), anodic (β_a) and cathodic (β_c) tafel slope. These measured parameters provide insights into the electrochemical behaviour of the steel rebars and their susceptibility to corrosion.

RESULTS AND DISCUSSION

Workability, compressive strength and microstructure of RGGPC

Workability of RGGPC

The slump value obtained for RGGPC mix was between 70 and 75 mm, as depicted in Figure 11. This indicates moderate workability, suitable for standard concrete placement and compaction practices. The consistency observed in the slump values suggests that the mix proportion effectively balances fluidity and cohesion, facilitating ease of handling and placement.

Figure 11. Slump cone test.

Compressive strength of RGGPC

The compressive strength test was carried on RGGPC specimens cast with the given mix proportion for both curing regimes. At the age of 28 days, the compressive strength was recorded as 35.8 MPa under heat curing and 32.5 MPa under ambient curing. The results were found to be satisfactory for the given mix proportion. The superior strength of heat-cured specimens can be attributed to enhanced geopolymerisation, which results in a denser and more compact matrix.

Microstructure of RGGPC
FT-IR

The FTIR spectrum of the ambient-cured sample sown in Figure 12a exhibited Si–O stretching vibrations between 900 – 1100 cm^{-1}, confirming the development of C–S–H and aluminosilicate phases. However, the intensity of these peaks was moderate, indicating an incomplete polymerisation process. The broad hydroxyl (-OH) stretching band at 3200 – 3500 cm^{-1} suggested a higher degree of bound water in the gel phase, indicating ongoing hydration and a slower reaction process. A peak at 1400 cm^{-1} was observed, indicating carbonate formation due to atmospheric CO_2 exposure, suggesting potential long-term carbonation effects. Also, a Si–O bending vibration was noted at 450–500 cm^{-1}, confirming silicate structure formation.

The FTIR spectrum of the heat-cured sample shown in Figure 12b displayed a stronger peak at 978 cm^{-1}, signifying a more developed aluminosilicate network and enhanced geopolymerisation. This suggests that elevated temperatures accelerate reaction kinetics, resulting in a denser and more chemically stable matrix. Peaks in the 3050 – 3600 cm^{-1} region correspond

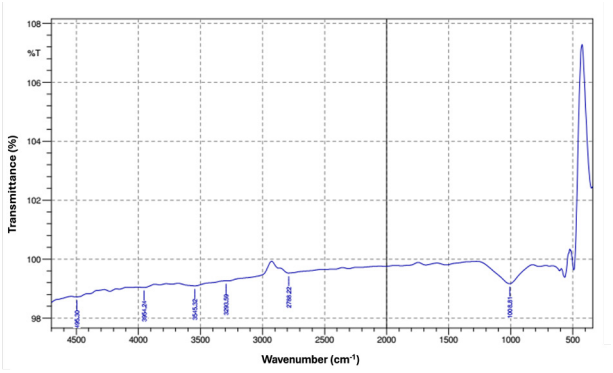

a) ambient curing

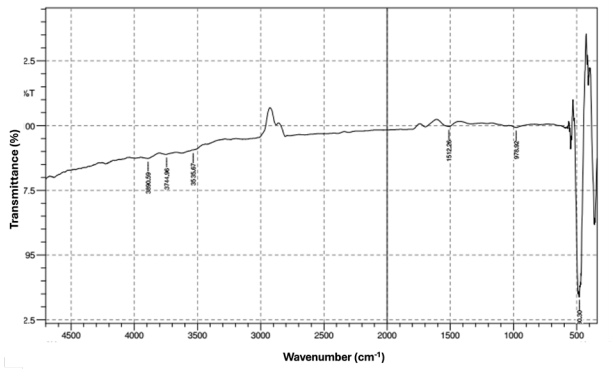

b) heat curing

Figure 12. FT-IR spectrum of the RGGPC.

to the stretching vibrations of hydroxyl (-OH) groups, which indicate the presence of chemically bound and absorbed water. The reduced hydroxyl peak intensity suggests lower water retention and improved polymerisation. This implies that heat curing effectively drives off excess moisture, resulting in a more compact and durable structure. The heat-cured sample exhibited a lower intensity carbonate peak at 1512 cm^{-1}, implying reduced atmospheric carbonation. This indicates that heat curing minimises external interactions, preserving the chemical stability of the geopolymer matrix. The Si–O bending vibration at 450 – 500 cm^{-1} was sharper and more defined, indicating a better-organised microstructure due to the enhanced polymerisation.

Thus, FTIR analysis demonstrates that heat curing significantly enhances the polymerisation and hydration processes compared to ambient curing. The heat-cured sample exhibits stronger aluminosilicate and C–S–H formation, lower bound water content, reduced carbonation effects, and more organized silicate structures, all of which contribute to an improved overall material.

SEM

The SEM image of the ambient-cured sample, as shown in Figure 13a, displays a porous and non-homogeneous microstructure, suggesting incomplete

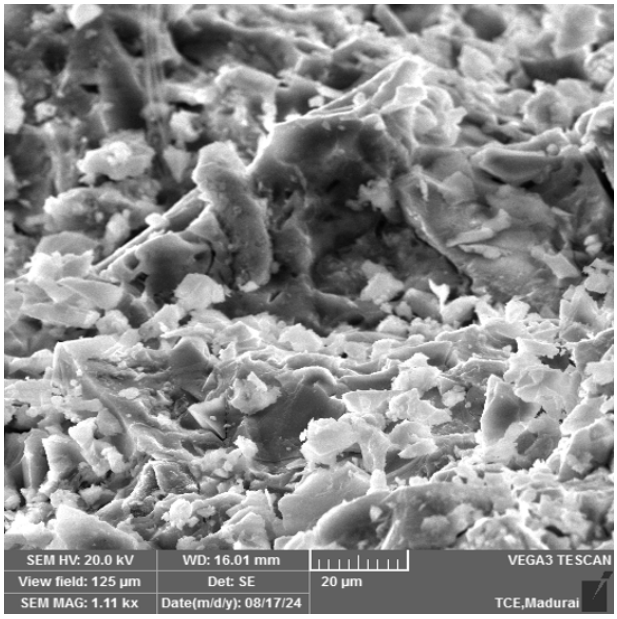

a) ambient curing

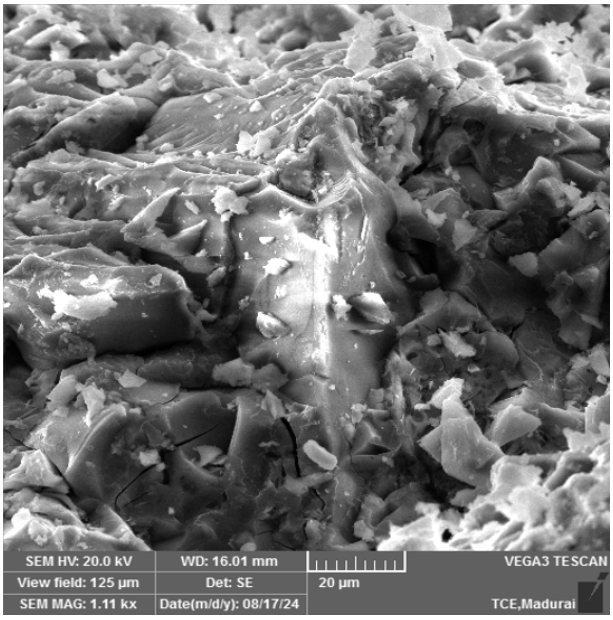

b) heat curing

Figure 13. SEM images of the RGGPC.

geopolymerisation. The presence of unreacted particles and weakly bonded phases indicates that the reaction process under ambient conditions was relatively slow, resulting in only partial dissolution of the raw materials. The SEM image indicates that the surface is rough and irregular and also, the formation of microcracks and voids, suggests lower matrix densification. Additionally, the loosely packed particles point to a less cohesive gel structure, which could negatively impact the mechanical strength and durability of concrete. This result aligns with the FTIR results, which confirm limited development of C–S–H and aluminosilicate phases and higher water retention, leading to slower hydration

and polymerisation. These findings suggest that ambient curing may require a longer duration to develop a well--structured and stable geopolymer matrix.

Figure 13b presents the SEM image of the heat-cured sample. From the image, it is clear that the microstructure is denser and more compact, which indicates enhanced geopolymerisation due to heat curing. The formation of a more cohesive and well-developed matrix is evident from the image, with fewer voids and microcracks compared to the ambient-cured sample. The smoother gel--like regions were seen in the figure, suggests improved dissolution of source materials and a higher degree of polymerisation lead to a well-connected aluminosilicate network. The reduced number of unreacted particles and the more uniform phase distribution further confirm that heat curing promotes efficient reaction kinetics. This compact microstructure is consistent with the FTIR results, which indicate stronger Si–O bonding, lower water retention, and reduced carbonation effects.

Rapid chloride penetration test

The chloride ion penetration test results for RGGPC are presented in Table 3. Based on ASTM C1202 classification, the electric charge transmitted to the specimens falls into the low categories. These categories indicate the level of chloride ion penetration, with low charges suggesting a relatively good resistance to chloride penetration. The extent of chloride ion ingress reflects the total charge passed into the concrete.

The results clearly indicate a gradual decline in the total charge passed through RGGPC specimens over time, with both heat-cured and ambient-cured samples. For all the test samples, the total charge passed decreased as the curing age increased.

A key observation from the results is the notable difference between heat curing and ambient curing. At 30 days, heat-cured samples recorded 1255 Coulombs, while ambient-cured samples showed 1421 Coulombs, indicating a 12 % lower charge passage in heat-cured specimens. This trend continued over time, with heat curing at 90 days reducing chloride penetration by approximately 20 % compared to 30 days, while ambient-cured samples exhibited a slightly lower improvement of about 15 % over the same period. The enhanced resistance in heat-cured samples is attributed to accelerated geopolymerisation, leading to a denser and more refined pore structure, which effectively limits the chloride ion transport.

The lower RCPT values in RGGPC can be explained by its compact microstructure and reduced ionic mobility [23]. Unlike ordinary Portland cement (OPC) concrete, where free ions present in the pore solution facilitate higher electrical conductivity, GPC forms a chemically stable aluminosilicate gel (N-A-S-H or C-A-S-H). This gel binds alkali ions, reducing their movement and, consequently, the overall charge passed in RCPT.

Furthermore, the results highlight that curing age significantly influences chloride penetration resistance. The progressive reduction in charge passed from 30 to 90 days suggests that continued geopolymerisation leads to further densification of the matrix, thereby reducing permeability and increasing durability over time. The heat-cured samples consistently outperformed the ambient-cured ones, reaffirming that elevated temperatures accelerate the formation of a refined, low--permeability structure.

Corrosion resistance of rebars

This research mainly focused on assessing the corrosion resistance characteristics of RGGPC through OCP and LPR tests, utilising an electrochemical workstation for analysis.

Table 3. RCPT results of the RGGPC.

Mix designation	Age in days	Charge Passed (Coulomb)		Category	
		Heat	Ambient	Heat	Ambient
R60G40	30	1255	1421	Low	Low
	60	1124	1212	Low	Low
	90	1004	1087	Low	Low

Open circuit potential test

One of the major problems in RC structures is the corrosion of rebars. The OCP test is widely used to find the likelihood of corrosion in steel reinforcement, a non-destructive method, without causing any damage to the structure. Conducted in compliance with ASTM C876, this test measures the OCP value, also referred to as E_{oc}. The OCP value serves as an indicator of the risk of corrosion. It is influenced by the condition of the steel rebar and the type of reference electrode used during measurement.

The test results shown in Figure 14 reveal that the R60G40 specimens subjected to ambient curing exhibited a high probability of corrosion (corresponding to a corrosion potential greater than -350 mV) and medium probability (between -350 and -200 mV).

Figure 14. OCP values of RGGPC.

In contrast, heat cured RGGPC specimens demonstrated medium to low corrosion probabilities, with corrosion potentials below -200 mV, by the classification criteria specified in ASTM C876 (1999). The test results of this research are consistent with the findings reported by Singh [24], that geopolymers offer enhanced protection for rebars against corrosion. Similarly, Farhana [25] highlighted that the steel reinforcement in GPC forms a robust silicate membrane that adheres firmly to the steel surface, effectively preventing rusting, even under neutral conditions. Thus, RGGPC specimens exhibit superior corrosion resistance properties.

Figure 14 highlights a strong correlation between the curing age and the corrosion resistance of rebars in RGGPC, irrespective of the curing method used. Initially, at 30 days of curing, the specimens displayed higher corrosion potential values. However, with longer curing durations, these values tend to decline. At 90 days of curing, RGGPC specimens exhibited significantly lower corrosion potential, which can be ascribed to significant enhancements in their internal structure. One of the primary factors contributing to this enhancement is using RHA and GGBS in the geopolymer matrix. The dense structure is an effective barrier against the ingress of harmful agents like NaCl. The probability of steel corrosion is greatly reduced by preventing these aggressive ions from reaching the embedded steel reinforcement. This observation aligns with the comparative outcomes of the RCPT test.

A comparison of curing methods reveals that specimens subjected to heat curing outperformed those cured under ambient conditions in terms of corrosion resistance. The heat-cured specimens consistently exhibited lower corrosion potential values, categorising them as having a minimal risk of corrosion. At 90 days, the open circuit potential (Eoc) for the heat-cured specimens was recorded at -172.64 mV, while specimens cured under ambient conditions displayed a higher potential of -278.03 mV. This enhanced performance in heat-cured specimens can be explained by the accelerated chemical reactions facilitated by elevated temperatures during the early curing ages. The accelerated reaction process results in the quick development of a compact and interconnected matrix of reaction products, including calcium-alumino-silicate-hydrate (C-A-S-H) gel. This gel significantly improves the structural integrity and impermeability of the concrete. Consequently, the concrete matrix becomes more resistant to the diffusion of aggressive ions, providing better protection to the embedded steel reinforcements.

In contrast, ambient curing, while effective to a degree, progresses at a slower rate and does not achieve the same level of microstructural refinement as heat curing. Consequently, ambient-cured specimens exhibit higher corrosion potential values than heat-cured specimens.

Linear polarisation resistance test

The OCP test has inherent limitations in quantitatively determining the rate of corrosion of rebars, as it is a qualitative method to evaluate the likelihood of corrosion of steel rebars. More advanced electrochemical techniques, such as Tafel polarisation analysis and LPR, are used to determine the corrosion rate of rebars embedded in RC.

In the LPR method, an electrical disturbance is applied to the reinforcement through surface of the concrete, allowing for the measurement of its polarisation resistance. This resistance is then used to assess the rate at which corrosion is occurring.

The corrosion rate of the RGGPC specimens was evaluated using the LPR technique for two curing methods. The polarisation curves are illustrated in Figure 15. The provided curves allow for determining two parameters: corrosion potential and corrosion

Table 4. Corrosion rate for the R60G40 mix.

Curing methods	Curing age in days	Corrosion current I_{corr} (μA)	Tafel slope (mV) Anodic β_a	Cathodic β_c	Rate of corrosion (mmpy)
Heat	30	14.81	301.0	262.0	0.0028
	60	10.38	315.2	290.9	0.0019
	90	9.04	324.8	268.6	0.0017
Ambient	30	46.82	316.7	285.1	0.0088
	60	42.62	316.4	291.2	0.0080
	90	13.56	329.8	256.0	0.0025

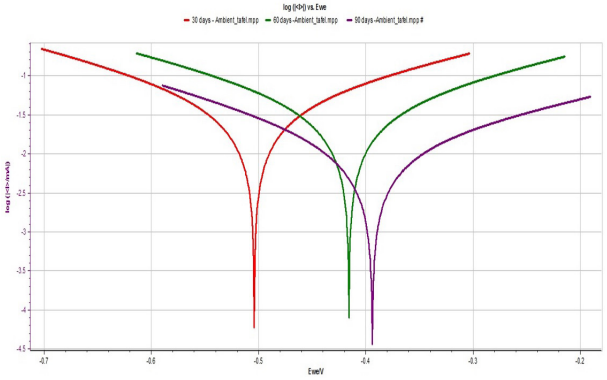

a) ambient curing

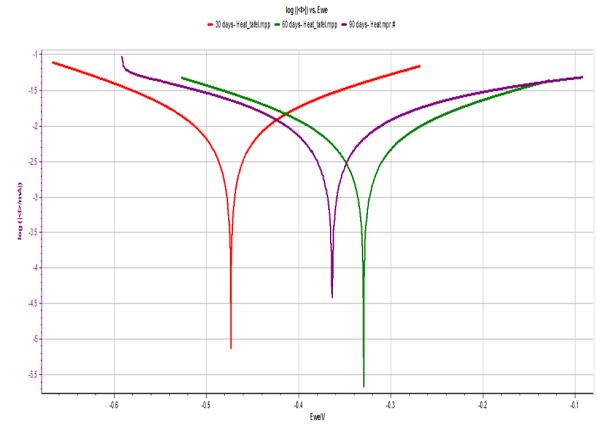

b) heat curing

Figure 15. Polarisation plots of the RGGPC.

current. These values are derived from the anodic and cathodic Tafel slopes, representing the respective electrochemical reactions occurring at the steel surface.

The experimental test values are presented in Table 4, which shows the corrosion performance of RGGPC specimens after curing for 30, 60 and 90 days under accelerated corrosion conditions. The results highlight the influence of curing duration and method on the corrosion resistance of RGGPC.

The corrosion behaviour of rebars embedded in the R60G40 specimens were evaluated under different curing conditions over varying curing ages. The results indicate a progressive reduction in corrosion rate with increased curing age, highlighting the role of microstructural refinement in enhancing durability. Additionally, heat-cured specimens consistently demonstrated lower corrosion rates than ambient-cured specimens, confirming the positive impact of heat curing on geopolymerisation.

At 30 days, the corrosion rate for heat-cured specimens was 0.0028 mm/year, while ambient-cured specimens exhibited a significantly higher rate of 0.0088 mmpy, representing a 214 % increase compared to heat curing. This substantial difference underscores the impact of temperature in accelerating the geopolymerisation process, resulting in a denser and more impermeable matrix. The lower charge passed in the RCPT for GPC, as reported earlier, further supports this observation, indicating reduced ionic mobility and chloride ingress due to the compact pore structure [26].

As the curing age increased, the corrosion resistance of both the heat-cured and ambient-cured specimens improved. By 60 days, the corrosion rate in the heat--cured specimens had reduced to 0.0019 mmpy, while the ambient-cured samples exhibited a lower reduction, reaching 0.0080 mmpy. This trend continued at 90 days, where the corrosion rate of the heat-cured specimens reached its lowest value of 0.0017 mmpy, while the ambient-cured specimens exhibited 0.0025 mmpy, representing a 32 % lower corrosion rate in the heat--cured specimens. These findings align with studies by Xu [27], who reported that slag in geopolymer concrete facilitates a prolonged geopolymerisation process, allowing for continued matrix densification over time. The hydroxyl buffering effect of slag sustains chemical reactions, leading to the gradual development of a more compact and durable microstructure, reducing both porosity and ionic mobility.

The superior corrosion resistance of the heat-cured specimens is further explained by the role of calcium in the GPC. Tennakoon [9] highlighted that high-calcium geopolymer concrete promotes the development of cross--linked calcium-alumino-silicate-hydrate (C-A-S-H) gels, which exhibit higher density and lower permeability compared to the non-cross-linked tobermorite-like calcium-silicate-hydrate (C-S-H) gels in ordinary Portland cement concrete. The enhanced matrix density of heat-cured specimens limits the chloride penetration and provides a higher degree of protection for steel reinforcement. This is evident from the RCPT results, where heat-cured GPC consistently exhibited lower charge values, indicating restricted ionic movement and improved resistance to chloride-induced corrosion.

Another significant factor influencing the corrosion resistance of GPC is oxygen depletion in the pore solution, particularly in slag-based mixes. In alkaline environments (such as GPC), sulfide ions (S^{2-}) react with oxygen (O_2) present in the pore solution. This oxidation reaction converts sulphide ions into elemental sulfur (S^0) or sulfate ions (SO_4^{2-}). As a result, dissolved oxygen is consumed, leading to a localised reduction in oxygen concentration in the concrete matrix. Since oxygen availability is a crucial factor in the cathodic reaction of corrosion, its depletion effectively slows down the corrosion process. The marked reduction in corrosion rates observed in heat-cured specimens suggests that this mechanism, combined with a dense, impermeable pore structure, plays a key role in limiting corrosion initiation and progression.

The combined effects of using GGBS and RHA in the development of GPC significantly improve its corrosion resistance. These materials contribute

to the refinement of the microstructure by enhancing the geopolymerisation process, and thereby mitigate corrosion through mechanisms such as oxygen depletion and the formation of dense gel structures. This makes GGBS and RHA valuable additions for achieving durable and corrosion-resistant concrete systems.

Correlation between the electrophysical properties and microstructure

For heat-cured RGGPC specimens, FTIR analysis shows sharper Si–O peaks, contributing to enhanced polymerisation, whereas SEM images reveal fewer microcracks and reduced porosity. This improved microstructure directly correlates with higher compressive strength, lower chloride penetration, and superior corrosion resistance at an early age. Over time, the electrical resistivity of heat-cured specimens increases, and chloride permeability decreases further, improving the long-term durability of the material. The presence of well-formed C-A-S-H gels restricts ionic movement, causing a substantial reduction in the corrosion rate. Thus, heat curing ensures superior mechanical and durability properties from an early stage, with continued improvement as the curing age increases.

In contrast, ambient-cured specimens exhibit a more porous and heterogeneous microstructure at an early age due to slower geopolymerisation. FTIR results indicate weaker Si–O vibrations, while SEM images show higher porosity and microcracking, contributing to lower initial strength, higher chloride permeability, and increased corrosion susceptibility. However, the performance of ambient-cured specimens is improved with an increase in curing age. The continued reaction of RHA and GGBS leads to progressive matrix densification, reduction in porosity, and, thereby, enhancement of the connectivity of reaction products. This is reflected in a gradual reduction in chloride ion ingress and improved corrosion resistance. By 90 days, ambient-cured specimens show a notable decrease in corrosion rate, though they remain slightly less durable than heat curing.

CONCLUSIONS

As a green and low-carbon cementitious material, geopolymers offer a promising solution to lower the resource depletion, energy consumption, and carbon dioxide emissions related with conventional building materials. The steel rebars reinforced in geopolymer concrete (GPC) have been thoroughly investigated for corrosion resistance using electrochemical methods. GPC is made with RHA, an agricultural by-product, and GGBS, an industrial by-product, were utilised as key components in the concrete mix. The compressive strength test results have unveiled that it is possible to use 60 % RHA and 40 % GGBS in the production of GPC. The key findings and conclusions from this experimental investigation are presented in this chapter.

The charge passed through the specimens is low for both the curing regimes and all the curing ages. The micro-filling effects of RHA and GGBS contribute to a denser microstructure, minimising chloride penetration.

According to ASTM standards, RGGPC demonstrates the lowest OCP value and is classified as negligible corrosion. This exceptional performance is a result of its enhanced microstructural characteristics.

RGGPC achieves the lowest corrosion rate, regardless of curing conditions and age. This is due to the increased polarisation resistance of the binder materials, which effectively reduces the corrosion of the rebars.

Heat curing at 60 °C significantly improved the early-age performance of RGGPC by accelerating the geopolymerisation process, leading to a stronger and more durable material. The heat-cured specimens consistently outperformed the ambient-cured ones in both chloride-ion penetration and corrosion resistance tests.

Thus, the study confirms that RHA and GGBS--based geopolymer concrete can be an effective solution for enhancing the durability and corrosion resistance of RC structures. The reduced chloride permeability and improved microstructure make it a viable alternative material for long-term performance in aggressive environments.

Acknowledgments

The Chairman and Principal of the Thiagarajar College of Engineering in Madurai, India, are gratefully acknowledged by the authors for their assistance in conducting the research. Here, the aid of the Material Testing Laboratory's teaching and non-teaching staff is also appreciated.

REFERENCES

1. Prusty J.K., Pradhan B. (2020): Effect of GGBS and chloride on compressive strength and corrosion performance of steel in fly ash-GGBS based geopolymer concrete. *Materials Today Proceeding, 32*, 850-855. doi: 10.1016/j.matpr.2020.04.210
2. Yilmaz A. (2021): Mechanical and durability properties of cement mortar containing waste pet aggregate and natural zeolite. *Ceramics-Silikáty, 65*(1), 48-57. doi: 10.13168/cs.2021.0001
3. Amran M., Al-Fakih A., Chu S.H., Fediuk R., Haruna S., Azevedo A., Vatin N. (2021): Long-term durability properties of geopolymer concrete: An in-depth review. *Case Studies in Construction Materials, 15,* e00661. doi: 10.1016/j.cscm.2021.e00661
4. Diaz-Loya E.I., Allouche E.N., Vaidya S. (2011):

Mechanical Properties of Fly-Ash-Based Geopolymer Concrete. *ACI Materials Journal, 108*, 300-306. doi: 10.14359/51682495

5. Almutairi A.L., Tayeh B.A., Adesina A., Isleem H.F., Zeyad A.M. (2021): Potential applications of geopolymer concrete in construction: A review. *Case Studies in Construction Materials, 15*, e00733. doi: 10.1016/j.cscm.2021.e00733
6. Tian Q., Sun S., Sui Y., Wang Y., Lv Z. (2021): Effects of composition of fly ash-based alkali-activated materials on compressive strength: A review. *Ceramics-Silikáty, 65,* 9-23. doi: 10.13168/cs.2020.0037
7. Sungkono K.K.D., Satyarno I., Priyosulistyo H., Perdana I. (2023): Corrosion Resistance of High Calcium Fly Ash Based Reinforced Geopolymer Concrete in Marine Environment. *Civil Engineering and Architecture, 11,* 3175-3189. doi: 10.13189/cea.2023.110827
8. Yeau K.Y., Kim E.K. (2005): An experimental study on corrosion resistance of concrete with ground granulate blast-furnace slag. *Cement and Concrete Research, 35,* 1391-1399. doi: 10.1016/j.cemconres.2004.11.010
9. Tennakoon C., Shayan A., Sanjayan J.G., Xu A. (2017): Chloride ingress and steel corrosion in geopolymer concrete based on long term tests. *Materials & Design, 116*, 287-299. doi: 10.1016/j.matdes.2016.12.030
10. Kumar M.P., Mini K.M., Rangarajan M. (2018): Ultrafine GGBS and calcium nitrate as concrete admixtures for improved mechanical properties and corrosion resistance. *Construction and Building Materials, 182*, 249-257. doi: 10.1016/j.conbuildmat.2018.06.096
11. Mei K., He Z., Yi B., Lin X., Wang J., Wang H., Liu J. (2022): Study on electrochemical characteristics of reinforced concrete corrosion under the action of carbonation and chloride. *Case Studies in Construction Materials, 17,* e01351. doi: 10.1016/j.cscm.2022.e01351
12. Panneerselvam V., Pazhani K.C. (2024): Experimental Studies on the Performance of Geo-Polymer Reinforced Concrete Beams Subjected to Accelerated Corrosion. *Polish Journal of Environmental Studies, 33*, 1357-1364. doi: 10.15244/pjoes/172757
13. Ganesan N., Abraham R., Deepa Raj S. (2015): Durability characteristics of steel fibre reinforced geopolymer concrete. *Construction and Building Materials, 93*, 471-476. doi: 10.1016/j.conbuildmat.2015.06.014
14. Olivia M., Nikraz H.R. (2011): Durability of Fly Ash Geopolymer Concrete in a Seawater Environment. In: *Proceedings of the Concrete 2011 Conference*, Oct 12 2011. Perth, WA: The Concrete Institute of Australia.
15. Shayan A., Xu A., Andrews-Phaedonos F. (2013): Field applications of geopolymer concrete: a measure towards reducing carbon dioxide emission. *Concrete in Australia, 39*(3), 34-44. https://www.researchgate.net/publication/284869336.
16. Ma Q., Nanukuttan S. V., Basheer P.A.M., Bai Y., Yang C. (2016): Chloride transport and the resulting corrosion of steel bars in alkali activated slag concretes. *Materials and Structures, 49*, 3663-3677. doi: 10.1617/s11527-015-0747-7
17. Wang W., Chen H., Li X., Zhu Z. (2017): Corrosion behavior of steel bars immersed in simulated pore solutions of alkali-activated slag mortar. *Construction and Building Materials, 143*, 289-297. doi: 10.1016/j.conbuildmat.2017.03.132.
18. Tittarelli F., Mobili A., Giosue C., Belli A., Bellezze T. (2018): Corrosion behaviour of bare and galvanized steel in geopolymer and Ordinary Portland Cement based mortars with the same strength class exposed to chlorides. *Corrosion Science, 134*, 64-77. doi: 10.1016/j.corsci.2018.02.014
19. Gunasekara C., Law D., Bhuiyan S., Setunge S., Ward L. (2019): Chloride induced corrosion in different fly ash based geopolymer concretes. *Construction and Building Materials, 200*, 502-513. doi: 10.1016/j.conbuildmat.2018.12.168
20. Krishnan R.I., Nagan S. (2022): Influence of zeolite on the concentration of alkaline activator in rice husk ash based geopolymer mortar. *Ceramics-Silikáty, 66*, 508-519. doi: 10.13168/cs.2022.0047
21. Hassani E.M, Vessalas K., Sirivivatnanon V., Baweja D. (2017): Influence of permeability-reducing admixtures on water penetration in concrete. *ACI Materials Journal, 114,* 911-922. doi: 10.14359/51701002
22. Lloyd N., Rangan B. (2010): Geopolymer Concrete with Fly Ash. In: *Second International Conference on Sustainable Construction Materials and Technologies*, 3, 1493-1504. Ancona, Italy: UWM Center for By-Products Utilization.
23. Mehta A., Siddique R. (2018): Sustainable geopolymer concrete using ground granulated blast furnace slag and rice husk ash: Strength and permeability properties. *Journal of Cleaner Production, 205*, 49-57. doi: 10.1016/j.jclepro.2018.08.313
24. Singh N.B., Middendorf B. (2020): Geopolymers as an alternative to Portland cement: An overview. C*onstruction and Building Materials, 237*, 117455. doi: 10.1016/j.conbuildmat.2019.117455
25. Farhana Z.F., Kamarudin H., Rahmat A., Mustafa Al Bakri A.M., Norainiza S. (2013): Corrosion performance of reinforcement bar in geopolymer concrete compare with its performance in ordinary portland cement concrete: A short review. *Advanced Materials Research, 795*, 509-512. doi: 10.4028/www.scientific.net/AMR.795.509.
26. Rengaraju S., Neelakantan L., Pillai R.G. (2019): Investigation on the polarization resistance of steel embedded in highly resistive cementitious systems - An attempt and challenges. *Electrochimica Acta, 308*, 131-141. doi: 10.1016/j.electacta.2019.03.200
27. Xu H., Deventer J.S.J.V. (2000): The geopolymerisation of alumino-silicate minerals. *International Journal of Mineral Processing, 59*, 247-266. doi: 10.1016/S0301-7516(99)00074-5